microPublication BIOLOGY

3/2/2024 - *Open Access*

Wounding increases nuclear ploidy in wound-proximal epidermal cells of the *Drosophila* pupal notum

James S. White[1,2], M. Shane Hutson[3,4§], Andrea Page-McCaw[1,2§]

[1]Dept. Cell and Developmental Biology, Vanderbilt University, Nashville, Tennessee, United States

[2]Program in Developmental Biology, Vanderbilt University, Nashville, Tennessee, United States

[3]Dept. Physics and Astronomy, Vanderbilt University, Nashville, Tennessee, United States

[4]Dept. Biological Sciences, Vanderbilt University, Nashville, Tennessee, United States

[§]To whom correspondence should be addressed: shane.hutson@vanderbilt.edu; andrea.page-mccaw@vanderbilt.edu

Abstract

After injury, tissues must replace cell mass and genome copy number. The mitotic cycle is one mechanism for replacement, but non-mitotic strategies have been observed in quiescent tissues to restore tissue ploidy after wounding. Here we report that nuclei of the mitotically capable *Drosophila* pupal notum enlarged following nearby laser ablation. Measuring DNA content, we determined that nuclei within 100 µm of a laser-wound increased their ploidy to ~8C, consistent with one extra S-phase. These data indicate non-mitotic repair strategies are not exclusively utilized by quiescent tissues and may be an underexplored wound repair strategy in mitotic tissues.

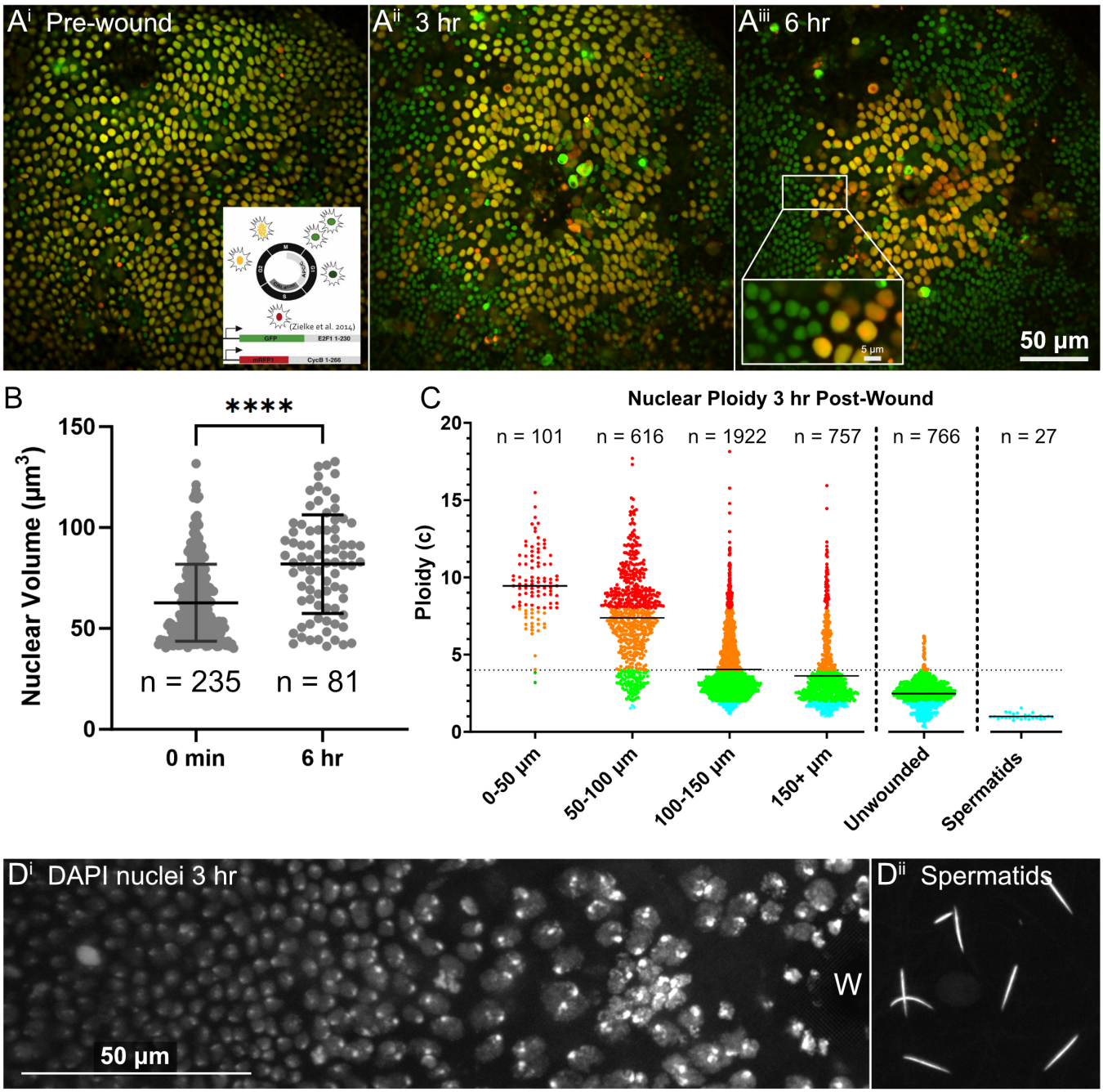

Figure 1. Wounding affects the cell-cycle and ploidy in the *Drosophila* pupal notum:

A: FUCCI fly indicating cell cycle state pre-wound, 3 hr, and 6 hr post wound in the *Drosophila* pupal notum (green nuclei = G1, red = S-phase, yellow = G2/M) Most nuclei are in G2 before wounding. Bar is 50 µm; inset bar in A^{iii} is 5 µm.

B: Nuclear volume of G2 (yellow) FUCCI nuclei segmented in 3D using NIS elements from 3 independent samples. Mean and standard deviation shown (black bars), Mann-Whitney test indicates $p < 0.0001$ (****) between 0 min and 6 hr post wounding.

C: DNA content of nuclei at 3 h after wounding. DAPI intensity was measured in 3D-segmented nuclei then normalized to DAPI intensity in haploid spermatids. Each dot represents a nucleus, and data from 4 biological replicates (wounded nota) are combined. Results are binned into 50 µm distances from wound center with *n* total nuclei within each bin shown. For reference, ploidy was measured in an unwounded control sample. Solid lines indicate the mean of each category, dotted line indicated 4C cutoff. A one-way ANOVA with multiple comparisons comparing the unwounded control to distance bins resulted in $p < 0.0001$ to each bin.

D: Nuclei increase in DNA content and size closer to the wound. **D^{i}** shows DAPI-stained nuclei 3 hr post-wounding. W=wound center. **D^{ii}** shows DAPI-stained spermatids used to normalize DNA content. Both images are max intensity projections, preprocessed with rolling ball correction before projection, 19 Z-slices in D^{i} and 24 Z-slices in D^{ii}. Bar is 50 µm and applies to D^{i} and D^{ii}.

Description

Epithelia maintain barriers to the outside environment, but after epithelial injury the loss of barrier integrity allows pathogens to invade. To re-establish the barrier and restore homeostasis, cells must cover the wound area. The mitotic cell cycle replaces cell mass as well as genetic material, and mitosis is observed in epithelial cells near a wound in mouse skin (Park et al., 2017). In the adult fly epidermis, however, epithelial cells are post-mitotic, and there is no stem cell pool to contribute new cells to close wounds. Previous studies have determined that in response to a wound, adult fly epidermal cells utilize endoreplication, which includes both growth (G) phases and S-phases but omits mitosis, resulting in larger cells with increased nuclear ploidy that close the wound (Losick et al., 2013; Losick et al., 2016). These large polyploid cells not only endocycle but also fuse with each other to form syncytia (Besen-McNally et al., 2021; Grendler et al., 2019; Losick et al., 2013; Losick et al., 2016). Similar non-mitotic repair strategies have been observed in other tissues (Cao et al., 2017; Edgar & Orr-Weaver, 2001; Gentric et al., 2015; González-Rosa et al., 2018; Lee et al., 2009; Orr-Weaver, 2015; Sigal et al., 1999; Wang et al., 2018; Wang et al., 2013; Wilkinson et al., 2019).

We have previously investigated wound responses in the *Drosophila* pupal notum (O'Connor et al., 2021; Shannon et al., 2017). Although this tissue is mitotic, we previously reported that epithelial cells near laser wounds fuse with their neighbors to form giant syncytia (White et al, 2023). Here, to investigate the cell-cycle response to wounds, we laser-ablated *Drosophila* pupae expressing the Fluorescent Ubiquitination-based Cell Cycle Indicator (FUCCI). FUCCI is designed to provide a live readout of cell-cycle state where green fluorescence from GFP-E2F1 corresponds to a cell in G1, red fluorescence from CycB-RFP corresponds to a cell in S-phase, and both fluorophores are present in G2/M. The epithelial cells of the unwounded pupal notum undergo waves of mitosis (Guirao et al., 2015); we wounded at 12-15h APF, when most cells were in G2 (yellow), some are in M (fluorophores lost after nuclear envelope breakdown) and G1 (green), with very few in S phase (red) (Fig. 1A^{i}). Post-wounding, wound-proximal nuclei did not progress through the cell cycle but rather maintained both fluorophores over the course of wound closure (Fig. 1 A^{ii},A^{iii}). Interestingly, at 6 h post wound, nuclei had an increased nuclear volume compared to immediately after wounding (Fig. 1B), suggesting these nuclei may be polyploid. To assess the ploidy of nuclei post-wound, we fixed and DAPI-stained the notum epithelium using a protocol we developed (White et al., 2022), normalizing to haploid spermatids that were fixed and DAPI-stained along with the dissected notum (Fig.1 D^{i}-D^{ii}). Within 3 h after wounding, nuclei within 100 µm from the wound averaged ~8C, consistent with one extra S-phase (Fig. 1C). In contrast, most nuclei further from the wound had ploidy levels within the diploid range, comparable to unwounded controls (Fig. 1C). Thus, even though the pupal notum epithelium is mitotic (Guirao et al., 2015; White et al., 2023), laser ablation induces nuclear polyploidy as well as cell fusion.

Previous studies investigating developmental polyploid cells using the FUCCI system observed green (G1) or red (S) nuclei, as expected for endoreplication (Burbridge et al., 2021; Wang et al., 2021); thus, it is noteworthy that we observed a different signature of both fluorophores together. However, these previous studies analyzed unwounded tissues. In the context of injury, a previous study using FUCCI indicated G2 stalling followed injury in the diploid cells of the *Drosophila* wing imaginal disc (Cosolo et al., 2019). It may be relevant that in our laser-ablation system, wound-proximal nuclei undergo significant damage after laser ablation (O'Connor et al., 2021). Most of these nuclei were in G2 when damaged, and they may not be able to execute mitosis in their damaged state, perhaps because they fail the G2/M checkpoint, or perhaps because the mechanical environment around the wound is not suited to mitosis (Han et al., 2023). Thus, these cells may enter S-phase directly, resulting in a different FUCCI signature than developmental polyploid cells. We note that the G1 (green) marker is based on E2F1, usually destroyed during S phase; but in mammals DNA damage activates and stabilizes E2F1 (Lin et al., 2001; Wang et al., 2004; Zhang et al., 2009), recruiting E2F1 to DNA damage sites (Choi & Kim, 2019). The role of E2F1 in the DNA damage response of *Drosophila*, however, has not been explored.

Our results indicate that even a mitotically active tissue can induce nuclear polyploidy in response to damage. Why would a mitotic tissue do this? Note that these wounds are healed rapidly, within 3-6 hours, and we speculate that polyploidization may increase both cell mass and the amount of genetic material faster than the available mitotic cell cycle in a damage context.

Methods

Flies:

Figure 1 A,B: w^{1118}; Kr^{If-1}/CyO, $P\{ry^{+t7.2}=en1\}wg^{en11}$; $P\{w^{+mC}=Ubi\text{-}GFP.E2f1.1\text{-}230\}5$ $P\{w^{+mC}=Ubi\text{-}mRFP1.NLS.CycB.1\text{-}266\}12/$ *TM6B,* Tb^{1} (Bloomington stock 55124)

Figure 1 C: *P{Ubi-p63E-shg.GFP}5 / CyO ; pnr-Gal4, UAS-mCherry.NLS, tubP-*$Gal80^{ts}$ */ TM3* (Flybase unique identifiers: FBti0004011, FBti0151829, FBti0147460, FBti0027797)

Wounding:

Flies were mounted and wounded as described previously (O'Connor et al., 2022; White et al., 2023).

Live imaging the cell cycle:

Cell cycles were visualized with the Fluorescent Ubiquitination-based Cell Cycle Indicator (FUCCI) fly (Zielke et al., 2014). Images were captured pre-wounding, immediately post-wound, and every ten minutes on a Nikon Ti2 Eclipse with X-light V2 spinning disc (Nikon, Tokyo, Japan) using a 60x oil-immersion objective.

Volume of FUCCI nuclei:

FUCCI nuclei with both E2F1-GFP and CycB-RFP were segmented in 3D using NIS Elements GA3. Brightspots segmentations were made for both E2F1-GFP and CycB-RFP and only nuclei that contained both fluorophores were analyzed to exclude the smaller G1 green-only nuclei. Volume measurements were performed both immediately after wounding and 6 h post-wound, exported to excel, and graphs were generated using GraphPad Prism 10.

DAPI staining and measurement:

ShgGFP / CyO ; PnrGal4, $Gal80^{ts}$*, UAS-nuc-mCherry / TM3* pupae were mounted, wounded, and allowed to recover for 3 h. Spermatids were dissected from healthy unwounded male flies and allowed to dry on a 24x60 mm coverslip. Two wounded pupae were isolated on the coverslip with dried spermatids, then dissected and fixed as previously described (O'Connor et al., 2022; White et al., 2022). Pelts and spermatids were incubated with 1 µg/ml DAPI for 45 min to allow the stain to completely penetrate the tissue, then washed and mounted as described previously (White et al., 2022).

DAPI intensity was assessed by creating an NIS elements macro to segment epithelial nuclei in a 3D volume. To create the segmentation macro, we used NIS elements General Analysis 3. Nuclei were segmented in 3D based on a nuclear-localizing mCherry fluorophore. mCherry signal was enhanced with the Local Contrast preprocessing and then segmented with Brightspots detection. Single voxel Brightspots were grown to fill the whole mCherry labeled nucleus. Nuclear segmentations were then filtered based on volume to exclude erroneously small and large objects, as well as sphericity to remove erroneously fused objects. Subtle variance in mCherry signal intensity across nuclei meant a single Brightspots setting would miss many nuclei. So, three Brightspots detections were run in parallel each with subtly different thresholding parameters to capture most nuclei. Outputs of the three Brightspots segmentations were merged into one binary image which was used to obtain DAPI intensity within nuclei. Some areas of DAPI stain were contaminated by an underlying bright muscle band signal. So, the DAPI channel was thresholded by eye for each sample so only nuclei within uncontaminated areas were included. Basal immune and blood cell nuclei are not entirely removed during dissection. To exclude these nuclei, only nuclei near the apical epithelial border marker E-cadherin GFP (ShgGFP) were analyzed. E-Cad GFP signal was refined with rolling ball and local contrast pre-processing and then thresholded to create a binary E-Cad sheet. The threshold was filtered by volume to remove small artifacts not connected to the E-Cad tissue sheet. The E-Cad Sheet was then dilated and only nuclei that fell within the dilated E-Cad sheet were analyzed. Nuclei were then assigned a distance from the wound bed by thresholding the dim E-Cad signal within the wound bed, which was refined by erosion and filtering by volume to leave only a single wound bed object. All nuclei were then assigned a distance from the center of the wound bed object. Finally, the sum intensity of the DAPI signal was determined for all nuclei collated with the distance from the wound and then output to a CSV file.

A 1C (haploid) standard was created by imaging spermatids on the slide with the same conditions as the pupae. Spermatids were thresholded and filtered by volume and elongation to remove erroneous objects. Sum DAPI intensity was taken for all filtered spermatids and exported as a CSV. Within the CSV, the average intensity of spermatids was determined, corresponding to a haploid genome or 1C. All nuclei intensity values were divided by the average spermatid value resulting in the ploidy in C for nuclei and their distance from the wound. Within the CSV nuclei were sorted by distance from the wound and exported to prism.

Acknowledgements:

We thank Kimi LaFever Hodge for technical assistance, Jasmine Su and Alex D. White for their assistance in generating ploidy graphs, and members of the Page-McCaw lab for helpful conversations. We thank the BDSC for fly stocks as well as

the Vanderbilt Nikon Center of Excellence past and present staff, Nicholas Mignemi and Kari Seedle, for lending their NIS elements expertise.

References

Besen-McNally R, Gjelsvik KJ, Losick VP. 2020. Wound-induced polyploidization is dependent on integrin-yki signaling. Biology Open : 10.1242/bio.055996. DOI: 10.1242/bio.055996

Burbridge K, Holcombe J, Weavers H. 2021. Metabolically active and polyploid renal tissues rely on graded cytoprotection to drive developmental and homeostatic stress resilience. Development 148: 10.1242/dev.197343. DOI: 10.1242/dev.197343

Cao J, Wang J, Jackman CP, Cox AH, Trembley MA, Balowski JJ, et al., Poss. 2017. Tension Creates an Endoreplication Wavefront that Leads Regeneration of Epicardial Tissue. Developmental Cell 42: 600-615.e4. DOI: 10.1016/j.devcel.2017.08.024

Choi EH, Kim KP. 2019. E2F1 facilitates DNA break repair by localizing to break sites and enhancing the expression of homologous recombination factors. Experimental & Molecular Medicine 51: 1-12. DOI: 10.1038/s12276-019-0307-2

Cosolo A, Jaiswal J, Csordás G, Grass I, Uhlirova M, Classen AK. 2019. JNK-dependent cell cycle stalling in G2 promotes survival and senescence-like phenotypes in tissue stress. eLife 8: 10.7554/elife.41036. DOI: 10.7554/eLife.41036

Edgar BA, Orr-Weaver TL. 2001. Endoreplication Cell Cycles. Cell 105: 297-306. DOI: 10.1016/s0092-8674(01)00334-8

Gentric G, Maillet V, Paradis V, Couton D, L'Hermitte A, Panasyuk G, et al., Desdouets C. 2015. Oxidative stress promotes pathologic polyploidization in nonalcoholic fatty liver disease. Journal of Clinical Investigation 125: 981-992. DOI: 10.1172/jci73957

González-Rosa JM, Sharpe M, Field D, Soonpaa MH, Field LJ, Burns CE, Burns CG. 2018. Myocardial Polyploidization Creates a Barrier to Heart Regeneration in Zebrafish. Developmental Cell 44: 433-446.e7. DOI: 10.1016/j.devcel.2018.01.021

Grendler J, Lowgren S, Mills M, Losick VP. 2019. Wound-induced polyploidization is driven by Myc and supports tissue repair in the presence of DNA damage. Development : 10.1242/dev.173005. DOI: 10.1242/dev.173005

Guirao B, Rigaud SU, Bosveld F, Bailles A, López-Gay J, Ishihara S, et al., Bellaïche Y. 2015. Unified quantitative characterization of epithelial tissue development. eLife 4: 10.7554/elife.08519. DOI: 10.7554/eLife.08519

Han I, Hua J, White JS, O'Connor JT, Nassar LS, Tro KJ, Page-McCaw A, Hutson MS. 2023. After wounding, a G-protein coupled receptor promotes the restoration of tension in epithelial cells. : 10.1101/2023.05.31.543122. DOI: 10.1101/2023.05.31.543122

Lee HO, Davidson JM, Duronio RJ. 2009. Endoreplication: polyploidy with purpose. Genes & Development 23: 2461-2477. DOI: 10.1101/gad.1829209

Lin WC, Lin FT, Nevins JR. 2001. Selective induction of E2F1 in response to DNA damage, mediated by ATM-dependent phosphorylation. Genes Dev 15(14): 1833-44. PubMed ID: 11459832

Losick VP, Fox DT, Spradling AC. 2013. Polyploidization and Cell Fusion Contribute to Wound Healing in the Adult Drosophila Epithelium. Current Biology 23: 2224-2232. DOI: 10.1016/j.cub.2013.09.029

Losick VP, Jun AS, Spradling AC. 2016. Wound-Induced Polyploidization: Regulation by Hippo and JNK Signaling and Conservation in Mammals. PLOS ONE 11: e0151251. DOI: 10.1371/journal.pone.0151251

O'Connor JT, Shannon EK, Hutson MS, Page-McCaw A. 2022. Mounting Drosophila pupae for laser ablation and live imaging of the dorsal thorax. STAR Protocols 3: 101396. DOI: 10.1016/j.xpro.2022.101396

O'Connor JT, Stevens AC, Shannon EK, Akbar FB, LaFever KS, Narayanan NP, et al., Page-McCaw. 2021. Proteolytic activation of Growth-blocking peptides triggers calcium responses through the GPCR Mthl10 during epithelial wound detection. Developmental Cell 56: 2160-2175.e5. DOI: 10.1016/j.devcel.2021.06.020

O'Connor J, Akbar FB, Hutson MS, Page-McCaw A. 2021. Zones of cellular damage around pulsed-laser wounds. PLOS ONE 16: e0253032. DOI: 10.1371/journal.pone.0253032

Orr-Weaver TL. 2015. When bigger is better: the role of polyploidy in organogenesis. Trends in Genetics 31: 307-315. DOI: 10.1016/j.tig.2015.03.011

Park S, Gonzalez DG, Guirao B, Boucher JD, Cockburn K, Marsh ED, et al., Greco V. 2017. Tissue-scale coordination of cellular behaviour promotes epidermal wound repair in live mice. Nature Cell Biology 19: 155-163. DOI: 10.1038/ncb3472

Shannon EK, Stevens A, Edrington W, Zhao Y, Jayasinghe AK, Page-McCaw A, Hutson MS. 2017. Multiple Mechanisms Drive Calcium Signal Dynamics around Laser-Induced Epithelial Wounds. Biophysical Journal 113: 1623-1635. DOI: 10.1016/j.bpj.2017.07.022

Sigal SH, Rajvanshi P, Gorla GR, Sokhi RP, Saxena R, Gebhard DR Jr, Reid LM, Gupta S. 1999. Partial hepatectomy-induced polyploidy attenuates hepatocyte replication and activates cell aging events. Am J Physiol 276(5): G1260-72. PubMed ID: 10330018

Wang B, Liu K, Lin FT, Lin WC. 2004. A role for 14-3-3 tau in E2F1 stabilization and DNA damage-induced apoptosis. J Biol Chem 279(52): 54140-52. PubMed ID: 15494392

Wang J, Batourina E, Schneider K, Souza S, Swayne T, Liu C, et al., Mendelsohn CL. 2018. Polyploid Superficial Cells that Maintain the Urothelial Barrier Are Produced via Incomplete Cytokinesis and Endoreplication. Cell Reports 25: 464-477.e4. DOI: 10.1016/j.celrep.2018.09.042

Wang Q, Wu PC, Dong DZ, Ivanova I, Chu E, Zeliadt S, Vesselle H, Wu DY. 2013. Polyploidy road to therapy-induced cellular senescence and escape. Int J Cancer 132(7): 1505-15. PubMed ID: 22945332

Wang XF, Yang SA, Gong S, Chang CH, Portilla JM, Chatterjee D, et al., Deng WM. 2021. Polyploid mitosis and depolyploidization promote chromosomal instability and tumor progression in a Notch-induced tumor model. Developmental Cell 56: 1976-1988.e4. DOI: 10.1016/j.devcel.2021.05.017

White JS, LaFever KS, Page-McCaw A. 2022. Dissecting, Fixing, and Visualizing the *Drosophila* Pupal Notum. Journal of Visualized Experiments : 10.3791/63682. DOI: doi:10.3791/63682

White JS, Su JJ, Ruark EM, Hua J, Shane Hutson M, Page-McCaw A. 2023. Wound-Induced Syncytia Outpace Mononucleate Neighbors during *Drosophila* Wound Repair. : 10.1101/2023.06.25.546442. DOI: 10.1101/2023.06.25.546442

Wilkinson PD, Alencastro F, Delgado ER, Leek MP, Weirich MP, Otero PA, et al., Duncan AW. 2019. Polyploid Hepatocytes Facilitate Adaptation and Regeneration to Chronic Liver Injury. The American Journal of Pathology 189: 1241-1255. DOI: 10.1016/j.ajpath.2019.02.008

Zhang YW, Jones TL, Martin SE, Caplen NJ, Pommier Y. 2009. Implication of checkpoint kinase-dependent up-regulation of ribonucleotide reductase R2 in DNA damage response. J Biol Chem 284(27): 18085-95. PubMed ID: 19416980

Zielke N, Korzelius J, van Straaten M, Bender K, Schuhknecht GFP, Dutta D, Xiang J, Edgar BA. 2014. Fly-FUCCI: A versatile tool for studying cell proliferation in complex tissues. Cell Rep 7(2): 588-598. PubMed ID: 24726363

Funding:

JSW was supported by National Institute of Child Health and Human Development T32HD007502. This work was supported by the National Institute of General Medical Sciences R01GM130130 to APM and MSH.

Author Contributions: James S. White: conceptualization, data curation, formal analysis, investigation, supervision, validation, visualization, writing - original draft. M. Shane Hutson: conceptualization, supervision, funding acquisition, formal analysis. Andrea Page-McCaw: conceptualization, funding acquisition, supervision, writing - original draft.

Reviewed By: Anonymous

Nomenclature Validated By: Anonymous

History: Received November 28, 2023 **Revision Received** February 28, 2024 **Accepted** February 29, 2024 **Published Online** March 2, 2024 **Indexed** March 16, 2024

Copyright: © 2024 by the authors. This is an open-access article distributed under the terms of the Creative Commons Attribution 4.0 International (CC BY 4.0) License, which permits unrestricted use, distribution, and reproduction in any medium, provided the original author and source are credited.

Citation: White, JS; Hutson, MS; Page-McCaw, A (2024). Wounding increases nuclear ploidy in wound-proximal epidermal cells of the *Drosophila* pupal notum. microPublication Biology. 10.17912/micropub.biology.001067